Astron. Astrophys. 360, 529–538 (2000)

ASTRONOMY AND ASTROPHYSICS

Photometric and integrated spectral study of the young open clusters Pismis 22, NGC 6178, NGC 6216 and Ruprecht 130⋆,⋆⋆

A.E. Piatti[1], **J.J. Clariá**[1], **and E. Bica**[2]

[1] Observatorio Astronómico, Laprida 854, 5000 Córdoba, Argentina
[2] Universidade Federal do Rio Grande do Sul, Depto. de Astronomía, CP 15051, Porto Alegre, 91500-970, Brazil

Received 4 April 2000 / Accepted 5 June 2000

Abstract. We present CCD observations in the B, V, and I passbands obtained for stars in the fields of the open clusters Pismis 22, NGC 6178, NGC 6216, and Ruprecht 130, projected not far from the Galactic centre ($|l| < 30°$, $|b| < 2°$). The sample consists of about 790 stars reaching down to $V \sim$ 18-19 mag. From the analysis of the colour magnitude diagrams, we confirmed the physical reality of the clusters and derived their reddening, distance and age. In addition, we obtained flux-calibrated integrated spectra in the range 3500–9200 Å for the cluster sample. The equivalent widths of the Balmer lines provided us with age estimates, while the comparison with template spectra allowed us to derive both foreground reddening and age. The photometric and spectroscopic results reveal that the four studied objects are young open clusters with ages ranging between 35 and 50 Myr. The clusters, located between 1.0 kpc and 4.3 kpc from the Sun, are affected by different amounts of interstellar visual absorption ($0.6 \simeq A_v \simeq 6.0$).

Key words: Galaxy: open clusters and associations: general – Galaxy: open clusters and associations: individual: NGC 6178, NGC 6216, Pismis 22, Ruprecht 130

1. Introduction

One of the most active fields in Galactic astrophysics is the study of the open cluster system. This is because open clusters are excellent laboratories from which, for instance, it is possible to place new constraints on the theoretical models of stellar evolution. The determination of open cluster parameters such as reddening, distance and age, is fundamental to understand their spatial distribution, which in turn can be used together with cluster metallicity information to examine the chemical evolution of the Galactic disk (see, e.g., Piatti et al. 1995, Twarog et al. 1997). Out of approximately 1200 objects presently catalogued as open clusters, only around 500 have some determination of their fundamental parameters (see, http://obswww.unige.ch/webda/). The remaining clusters have not been studied in detail yet, mainly because they are either relatively faint objects or located in obscured and/or crowded fields.

The present work is part of a systematic photometric and spectroscopic survey of mostly unstudied open clusters (or candidates), preferably located towards the central parts of the Galaxy (Piatti et al. 1999 and references therein), with the aim of: (1) To decide whether the studied objects constitute genuine physical systems or, contrarily, the apparent concentration of stars in a region is consequence of the random fluctuation in the stellar density of that zone. (2) To determine ages, distances, reddenings and metallicities of those objects confirmed as open clusters. (3) To improve and enlarge the results of Piatti et al. (1995), with respect to the existence and size of the radial and perpendicular metal abundance gradients and the age-metallicity relationship for the disk of our Galaxy, using a longer baseline in Galactocentric distances.

In this paper we present the results obtained for the following clusters: Pismis 22 (OCI-957, α_{1950}=$16^h09^m.6$, δ_{1950}=-51°47′; l=331°.36, b=-0°.55), NGC 6178 (OCI-980, α_{1950}=$16^h32^m.1$, δ_{1950}=-45°32′; l=338°.40, b=+1°.23), NGC 6216 (OCI-989, α_{1950}=$16^h45^m.8$, δ_{1950}=-44°39′; l=340°.67, b=+0°.01) and Ruprecht 130 (OCI-1034, α_{1950}=$17^h44^m.4$, δ_{1950}=-30°06′; l=359°.22, b=-0°.98). Only Pismis 22 and NGC 6178 have some previous information available. In the case of Pismis 22, Westerlund (1969) published UBV photoelectric and photographic observations for 10 and 29 stars, respectively, located near and in the field of the small emission nebula RCW 103 (G332.4-0.4, PKS 1613-50). This nebula is now known to be a supernova remnant at an estimated distance of 6.6 kpc (Ilovaisky & Lequeux 1972, van den Bergh 1978). Westerlund identified the stars as part of an anonymous cluster but he did not derive any cluster parameter. On the other hand, Moffat & Vogt (1973, hereafter MV73) reported UBV photometry of 19 stars in the field of NGC 6178 and estimated a mean reddening E(B-V)=0.24 and an apparent distance modulus of 10.55 mag, which

Send offprint requests to: A.E. Piatti (andres@mail.oac.uncor.edu)

⋆ Based on observations made at Complejo Astronómico El Leoncito, which is operated under agreement between the Consejo Nacional de Investigaciones Científicas y Técnicas de la Repúbica Argentina and the National Universities of La Plata, Córdoba, and San Juan, Argentina, and at the University of Toronto (David Dunlap Observatory) 24-inch telescope, Las Campanas, Chile.

⋆⋆ Tables 3–6 are only available in electronic form at the CDS via anonymous ftp to cdsarc.u-strasbg.fr (130.79.128.5) or via http://cdsweb.u-strasbg.fr/Abstract.html

Table 1. Journal of observation.

Photometric data				
Object	Date (UT)	Filter	Exposures	seeing ($''$)
Pismis 22	1995 June 27	B	2x60 sec, 2x900 sec	1.5
		V	1x60 sec, 2x600 sec	1.6
		I	2x5 sec, 1x10 sec, 1x60 sec	1.4
NGC 6178	1995 July 1	B	1x20 sec, 1x40 sec, 1x120 sec	1.5
		V	2x10 sec, 1x50 sec	1.3
		I	1x2 sec, 1x4 sec, 1x20 sec	1.2
NGC 6216	1995 June 28	B	1x60 sec, 2x600 sec	1.6
		V	1x60 sec, 2x400 sec	1.5
		I	1x60 sec, 2x180 sec	1.4
Ruprecht 130	1995 July 3	B	2x900 sec	1.8
		V	1x480 sec, 1x600 sec	1.8
		I	1x20 sec, 1x60 sec, 1x50 sec	1.8

Spectroscopic data				
Object	Date (UT)	Spectral range	Exposures	S/N
Pismis 22	1995 May 25	blue	4x900 sec	31
	1995 May 28	red	4x900 sec	20
NGC 6178	1995 May 20	blue	3x900 sec	57
	1995 May 23	red	3x900 sec	48
NGC 6216	1995 May 20	blue	4x900 sec	32
	1995 May 23	red	4x900 sec	21
Ruprecht 130	1995 May 27	blue	2x900 sec	18
	1995 May 29	red	3x900 sec	44

in turn leads to a distance of 0.91 kpc. Later, FitzGerald et al. (1979) obtained objective prism spectra for 8 of the 19 stars of MV73 and derived their MK types. Seven of these stars turned out to be B1-B8 stars belonging to the Main Sequence (MS) of the cluster. NGC 6178 also served us as a control cluster, particularly to check the zero points of the CCD magnitude scale.

This paper is structured as follows: in Sect. 2 we present the observations and describe the reduction procedures briefly. In Sects. 3 and 4 we derive reddening, distance and age of the cluster sample from the photometric and spectroscopic data, respectively. We discuss the adopted cluster parameters in Sect. 5, and finally we summarize the main conclusions of this work in Sect. 6.

2. Observations and reductions

We obtained CCD BVI images in the fields of Pismis 22, NGC 6178, NGC 6216 and Ruprecht 130 during 4 photometric nights in June-July 1995, with the 24-inch telescope of the University of Toronto Southern Observatory, situated at Las Campanas Observatory, Chile. A PM 512x512 METACHROME CCD coated to give improved blue response was used, covering a total field of about $4'$x$4'$ ($0''.45$ per pixel). Columns (4) and (5) of Table 1 list the exposure sequences and the typical seeing for each object and filter, while Fig. 1 shows the schematic finding charts built with all the measured stars in the V band. We also nightly observed an average of 12 standard stars located in the

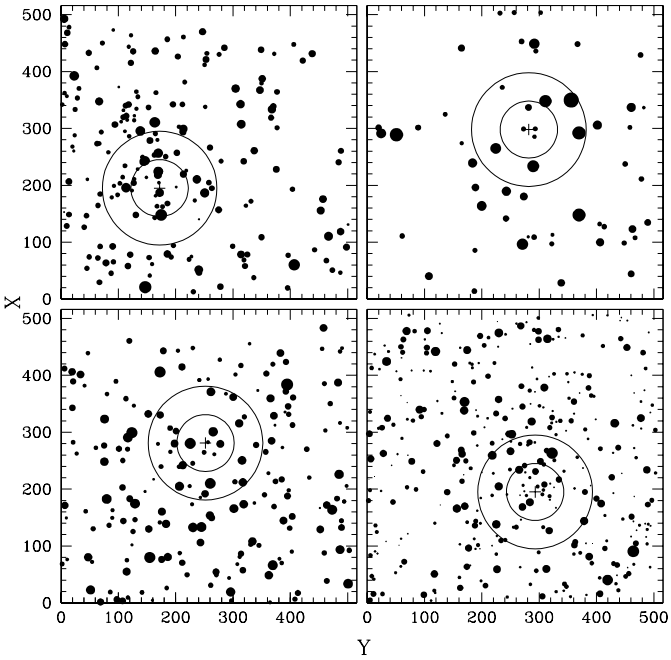

Fig. 1. Schematic finding charts for the fields of Pismis 22 (top-left), NGC 6178 (top-right), NGC 6216 (bottom-left), and Ruprecht 130 (bottom-right). A cross indicates the adopted cluster centre. Two concentric circles of $22''.5$ and $45''.0$ radii are also shown. North is up and East is to the left. The sizes of the plotting symbols are proportional to the brightness of the stars.

fields SA 104, 105, 107, 110, 111 and 112 (Landolt 1992) to transform to the standard system. Finally, we took a series of 10 bias and 10 skyflat frames during the sunsets and 10 domeflat frames at the end of each night for CCD calibration purposes. The airmass values for both program and standard fields were always smaller than 1.2.

The observations were reduced at the Astronomical Observatory of the National University of Córdoba, Argentina, using the IRAF[1] routines. The instrumental magnitudes were obtained through the DAOPHOT package as follows: first, we performed aperture photometry using a 4 pixel aperture radius on all the identified stars by DAOFIND. Then, we built the Point Spread Function (PSF) of a given frame from 15–20 selected stars and simultaneously fitted it on all the identified stars in that frame. Then, we applied aperture corrections to set the zero point of the PSFs to the values that they would have if the aperture photometry of the PSF stars had been done with an aperture similar to that used for standard stars (16 pixel aperture radius). Atmospheric extinction was removed with the coefficients from Vázquez et al. (1996). The resulting instrumental magnitudes b, v and i were transformed to the standard system from the following relations:

$$b_{j,n} = b_1 + V + (B-V) + b_2(B-V), \quad (1)$$

$$v_{k,n} = v_1 + V + v_2(B-V), \quad (2)$$

$$i_{l,n} = i_1 + V - (V-I) + i_2(V-I), \quad (3)$$

where V, $(B-V)$ and $(V-I)$ are the standard magnitude and colours. Note that for each night n there are as many instrumental magnitudes per filter as observed stars, so that Eqs. (1) to (3) were fitted by least squares simultaneously, the rms errors being 0.010, 0.009 and 0.011, respectively. The resulting coefficient values and associated errors are listed in Table 2. Then, we used these equations to derive the magnitude and colours of all the stars measured for each independent BVI filter set, and combined all the independent magnitudes and colours by building a final table per program field. These tables list for each star the X and Y coordinates, the V magnitude, the $B-V$ and $V-I$ colours, the number of observations n, and the standard deviations $\sigma(V)$, $\sigma(B-V)$, and $\sigma(V-I)$, computed from the n independent values. This procedure allowed us to obtain the individual photometric internal errors as well as to detect any anomalous value. Tables 3 to 6(a) and (b) provide this information and are available in electronic form at the CDS via anonymous ftp to cdsarc.u-strasbg.fr. A comparison of our CCD magnitude and colour scales with that of MV73 for 16 stars in common in NGC 6178 yields: $\Delta(V_{MV73}-V_{CCD}) = 0.001 \pm 0.023$ and $\Delta((B-V)_{MV73}-(B-V)_{CCD}) = 0.005 \pm 0.029$, which shows that our photometry agrees well with the MV73's photoelectric scale.

[1] IRAF is distributed by the National Optical Astronomy Observatories, which is operated by the Association of Universities for Research in Astronomy, Inc., under contract with the National Science Foundation.

Table 2. Transformation coefficients.

Date (UT)	b_1	b_2	v_1	v_2	i_1	i_2
1995 June 27	7.246	-0.081	7.023	-0.012	6.509	-0.116
	±0.009	±0.006	±0.011	±0.010	±0.010	±0.011
1995 June 28	7.280	-0.074	7.049	-0.016	6.587	-0.085
	±0.013	±0.011	±0.013	±0.013	±0.012	±0.011
1995 July 1	7.244	-0.073	7.014	-0.022	6.532	-0.090
	±0.010	±0.005	±0.009	±0.009	±0.012	±0.012
1995 July 3	7.256	-0.085	7.053	-0.019	6.531	-0.075
	±0.011	±0.006	±0.010	±0.011	±0.013	±0.012

The integrated spectroscopic observations were carried out with the 2.15 m telescope at the Complejo Astronómico El Leoncito (CASLEO, Argentina) during a run in May 1995. We employed a REOSC spectrograph containing a Tektronics CCD of 1024x1024 pixels, the size of each pixel being 24x24 μm. The slit was oriented in the east-west direction and the observations were made by scanning the slit across the objects in the north-south direction in order to get a proper sampling of cluster stars. The total field along the slit was $4'.7$ and, consequently, we could sample background regions. A grating of 300 lines/mm was used in two different set-ups, namely "blue nights" and "red nights". During the blue nights, we obtained spectra ranging from 3500 to 7000 Å with an average dispersion in the observed region of 140 Å/mm (3.46 Å/pixel). The slit width was $4''.2$ resulting in an average resolution of 14 Å, according to the FWHM of the He-Ar comparison lamps. During the red nights, we obtained spectra from 5800 to 9200 Å with a similar dispersion (3.36 Å/pixel) and a resolution of 17 Å (same slit width). In addition, to eliminate second order contamination an OG 550 filter was employed. We took exposures of 15 minutes each with a total exposure time ranging between half an hour and an hour per cluster, depending on the surface brightness of the objects, the sky conditions and the S/N ratio of each spectrum. The log for the spectroscopic observations is given in Table 1. S/N ratios were measured in regions of 300–500 Å wide, relatively free from absorption and emission lines. We also observed spectrophotometric standards to derive flux calibrations. Stars LTT 4364, EG 274 and LTT 7379 (Stone & Baldwin 1983) were used in the blue range. In the red range, the hot dwarf star HD 160233 (Gutiérrez-Moreno et al. 1988) was added to the standard list, which allowed us the correction for telluric absorption bands. Frames of He-Ar comparison lamps between and after the object observations, bias and dome, twilight sky, and tungsten lamp flat-fields were also taken.

The integrated spectra were reduced at the Astronomical Observatory of Córdoba in the standard way within the IRAF environment. First, we subtracted the bias and used previously combined flat field frames to correct the frames for high and low spatial frequency variations. Then, we applied background sky subtraction using pixel rows from the same frame, after having cleaned the background sky regions from cosmic rays. We checked that no significant background residuals were present on the resulting spectra. The cluster spectra were extracted and

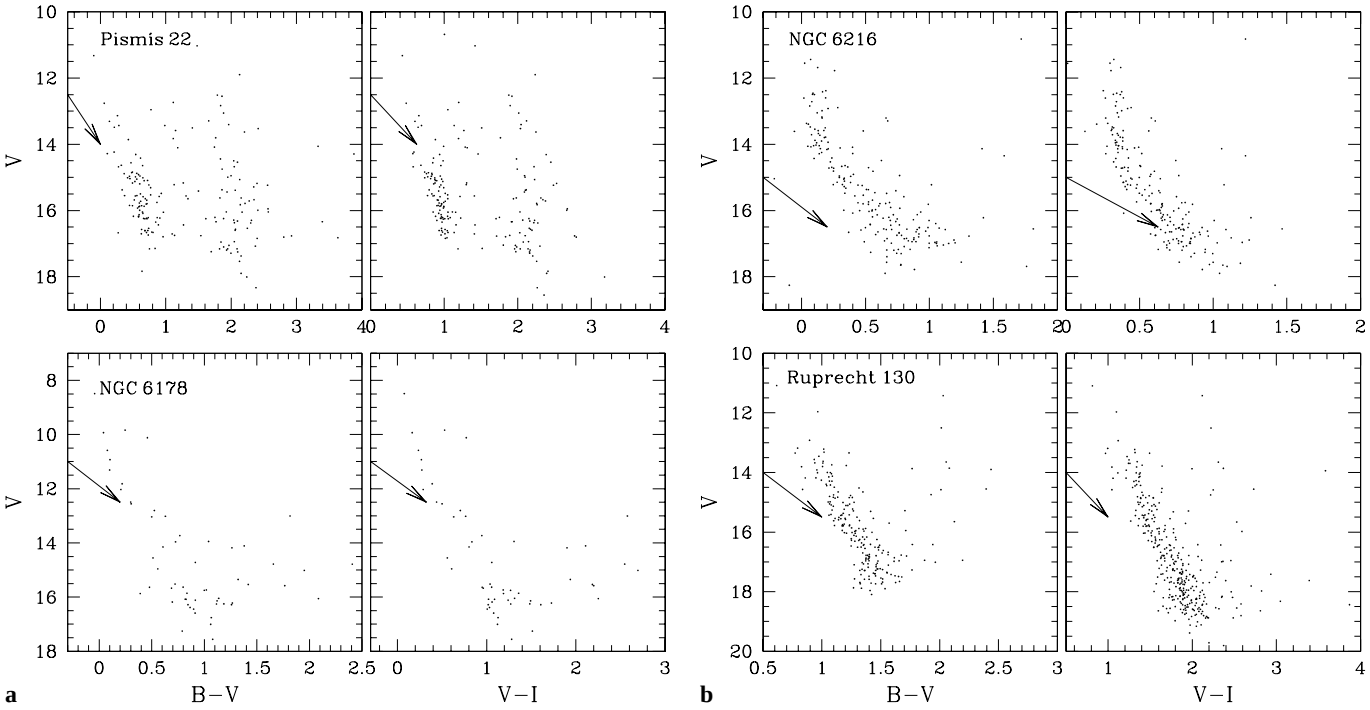

Fig. 2. a (V,$B-V$) and (V,$V-I$) diagrams of stars in the fields of Pismis 22 (top) and NGC 6178 (bottom); **b** (V,$B-V$) and (V,$V-I$) diagrams of stars in the fields of NGC 6216 (top) and Ruprecht 130 (bottom). The direction and size of the reddening vector for E(B-V)=0.5 mag, assuming A_v=3.0E(B-V) and E(V-I)=1.25E(B-V), are also shown.

Table 3. Magnitudes and colours of stars in the field of Pismis 22.

ID	$X_{\rm pixels}$	$Y_{\rm pixels}$	V	$\sigma(V)$	$B-V$	$\sigma(B-V)$	$V-I$	$\sigma(V-I)$	
1	392.312	22.973	13.337	0.021	1.515	0.017	1.597	0.012	3
2	63.644	78.483	15.234	0.025	0.721	0.014	1.083	0.021	3
3	92.625	90.085	15.477	0.011	0.957	0.017	1.231	0.006	3
4	306.712	94.007	15.488	0.028	0.765	0.023	1.159	0.028	3
5	295.513	138.264	13.149	0.011	2.260	0.002	2.320	0.014	2
⋮	⋮	⋮	⋮	⋮	⋮	⋮	⋮	⋮	⋮

NOTE: Tables 3 to 6 are available in its entirety in electronis form at the CDS via anonymous ftp to cdsarc.u-strasbg.fr. A portion of Table 3 is shown here for guidance regarding its form and content.

calibrated in wavelength by fitting He-Ar comparison lamp spectra with template spectra. The mean rms errors involved in these calibrations are 0.74 Å (0.21 pixel) and 0.45 Å (0.13 pixel) for blue and red nights, respectively. Once the wavelength calibrations were derived, we applied to the cluster spectra extinction corrections and flux calibrations, derived from the observed standard stars. Finally, we eliminated the telluric absorption bands in the near-IR dividing the program spectra by [1-(1-atm)*K], where atm is the normalization spectrum and K a factor around the unity. Thus, the intensity of the absorption bands in the normalization spectrum were scaled to those in the program spectra.

3. Photometric analysis

The ($V, B-V$) and ($V, V-I$) Colour-Magnitude Diagrams (CMDs) of the selected objects are shown in Figs. 2a and b. The observed ($V, V-I$) diagram of Ruprecht 130 presents more stars than that based on the $B-V$ colour, which is mainly due to reddening effects. The CMDs of NGC 6178, NGC 6216 and Ruprecht 130 reveal well defined sequences with relatively few stars lying outside them. In particular, the envelopes of the upper part of the CMDs do not seem to follow the direction of the reddening vector, but resemble the MSs of relatively young open clusters. On the other hand, the CMDs of Pismis 22 appear dominated by two star sequences, the bluer sequence being more populous and slightly more tilted. Consequently, from a quick look at these CMDs it is difficult to recognize which of both sequences might correspond to a cluster. Moreover, stars which appear concentrated in a small area of the sky do not necessarily form a cluster, but can be distributed at different distances in the same line of sight. Precisely, the loci in the CMDs of stars located in the innermost part of such group of stars, allow us to

decide whether they constitute a genuine system and, in such a case, to trace the fiducial cluster sequence and avoid possible non-physical members. In fact, the broadness of the MSs may be either an intrinsic characteristic of the cluster or caused by field star contamination and/or variable reddening.

In order to obtain the CMDs for the core regions of these four objects, we first determined their centres, and then made CMDs for circular extractions of the stars distributed within 50 (22′.5) and 100 (45′.0) pixels, respectively, around the central positions. The positions of the centres were estimated bearing in mind both the peaks in the star density profiles in the X and Y directions and the geometrical centres taken from the corresponding finding charts. The adopted positions of the centres of Pismis 22, NGC 6178, NGC 6216 and Ruprecht 130 are (X_c, Y_c) = (195,172), (298,282), (281,252) and (195,293), respectively. Fig. 1 shows the adopted centres as well as two concentric circles of 50 and 100 pixel radii. The size of these two circular extractions represent a compromise between the necessary number of stars to define the fiducial cluster sequence and a critical radius from which the contamination of field stars becomes important.

Figs. 3a and b show the CMDs for both circular extractions. Stars within 50 and 100 pixel radii are represented by filled circles and crosses, respectively, while those distributed outside the 100 pixel radius are represented with dots. From the two apparent sequences in the field of Pismis 22, the reddest one seems to correspond to the cluster as most of the stars in the core region (filled circles and crosses) define it. This sequence, with brighter and fainter stars, spreads over a wider magnitude range than the blue sequence and is not parallel to the reddening vector. The apparent steepness of this sequence suggests that we are also dealing with a young cluster. The bluer field star sequence can arise from stars at almost exactly the same distance, stars of very similar spectral classes, stars subject to different amounts of reddening, or these three conditions combined. Ng et al. (1996) studied the contribution of stars from the disk and bulge population to CMDs of star fields located at low Galactic latitudes in the direction to the Galactic centre. They identified the regions of the CMDs where disk and bulge stars are located. According to their findings, the blue star sequence in the CMD of Pismis 22 is formed by MS disk stars. Similar MS disk star sequences have been observed by Piatti et al. (1998a, 1998b) in the directions towards the open clusters Pismis 19 and Westerlund 1, respectively. Appart from confirming that there are cluster stars distributed all over the observed fields, the CMDs of the other three clusters do not provide additional information. An inspection of Figs. 3a and b reveals that the cluster MSs are, in general, tighter than the observed sequences. In particular, the circular extractions in the field of NGC 6178 include few stars, because this is the observed cluster with the lowest star density (see Fig. 1). Note that the CMDs of Ruprecht 130 with the larger circular extraction (Fig. 3b, cross symbols) include a star with V = 11.424, $B-V$ = 2.030 and $V-I$ = 2.119 which, in case of being a cluster member, could result in an evolved star during the short phase in the evolution of the young cluster, like an asymptotic giant star with a massive progenitor (BA86b, Renzini and Buzzoni 1985). CMDs for cluster fields located approximately towards a similar direction as that of the present cluster sample were recently published by Piatti et al. (1998c, 1999) and Sung et al. (1998), the former using the same techniques as in this work. Their CMDs reveal that at the distance of the studied clusters, which are distributed between 1.0 and 3.0 kpc from the Sun, there is no evidence for the presence of hundreds or even thousands of field stars, the variation in the stellar density being the most noticeable characteristic. Precisely, they found that both stars not uniformly distributed and abrupt changes in interstellar absorption are main features of this region of the Galactic disk.

Table 7. Cluster fundamental parameters derived from the CMDs analysis.

Cluster	E(B-V)	σ	E(V-I)	σ	V-M$_v$	σ	Age (Myr)
Pismis 22	2.00	0.10	2.10	0.10	16.00	0.50	5–50
NGC 6178	0.20	0.05	0.30	0.05	10.50	0.25	50
NGC 6216	0.45	0.05	0.55	0.05	14.50	0.25	50
Ruprecht 130	1.20	0.05	1.55	0.05	15.25	0.25	50–100

Cluster reddenings and distances were then derived by matching the fiducial cluster sequences in the $(V, B-V)$ and $(V, V-I)$ planes to the Zero Age Main Sequences (ZAMSs) of Schmidt-Kaler (1982) and Piatti et al. (1998c), respectively. Cluster ages were estimated from the empirical isochrones traced by Piatti et al. (1998c) in the M_v vs $(V-I)_o$ diagram, which cover ages from 5 up to 4000 Myr. Since $(V-I)_o$ is virtually free from metallicity effects (Rosvick 1995, Kassis et al. 1996), these isochrones are particularly useful to derive ages of highly reddened open clusters regardless of their metallicity. The matching was performed using all the measured stars in each field, but assigning more weight to the stars within the circular extractions. Taking into account that it is possible to change reddening and distance modulus simultaneously and even obtain a satisfactory fitting, we decided to use as reference the E(B-V) colour excesses and ages provided by the spectroscopic analysis (see Sect. 4). Fig. 4 shows the best match we found for the four clusters, whereas Table 7 presents the resulting E(B-V) and E(V-I) colour excesses and apparent distance moduli. The E(V-I)/E(B-V) ratio for these four clusters resulted in 1.3±0.1, which indicates that the interstellar absorption towards the clusters follows approximately the normal extinction law.

4. Spectroscopic analysis

Reddening, age and metallicity determinations for galactic open clusters have been mostly based on CMDs and/or photometric studies of individual giants (see, e.g., Hagen 1970, Janes et al. 1988, Meynet et al. 1993, Clariá et al. 1999). However, integrated spectra of relatively compact star clusters from which it is difficult to gather information about stars unaffected by contamination, can also provide valuable independent information about reddening, age and metallicity (see, e.g., Santos & Bica

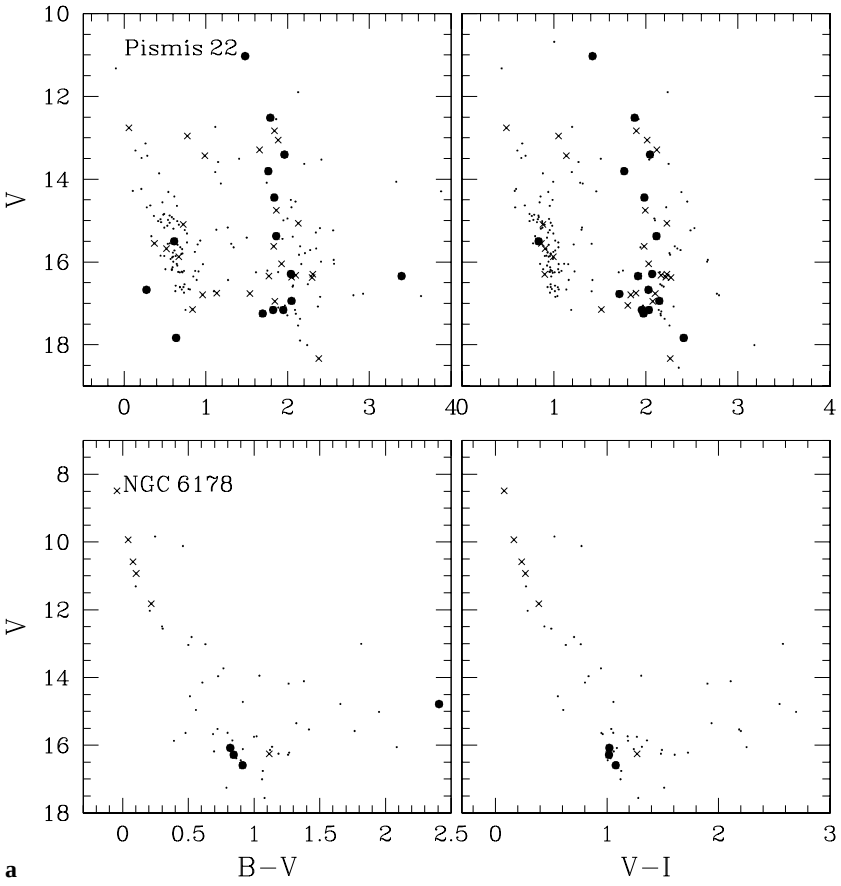

a

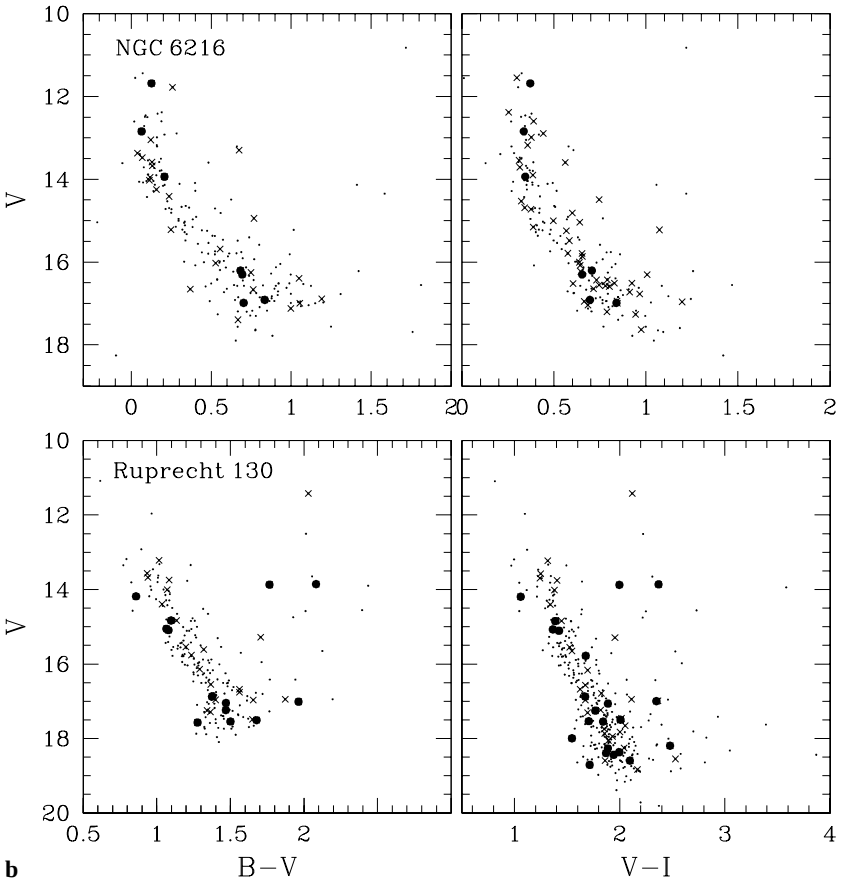

b

Fig. 3. **a** Colour-magnitude diagrams of stars in the field of Pismis 22 (top) and NGC 6178 (bottom): all measured stars (dots), circular extraction for r<22″.5 (filled circles) and r<45″.0 (crosses) are superimposed; **b** Colour-magnitude diagrams of stars in the fields of NGC 6216 (top) and Ruprecht 130 (bottom): symbols same as **a**.

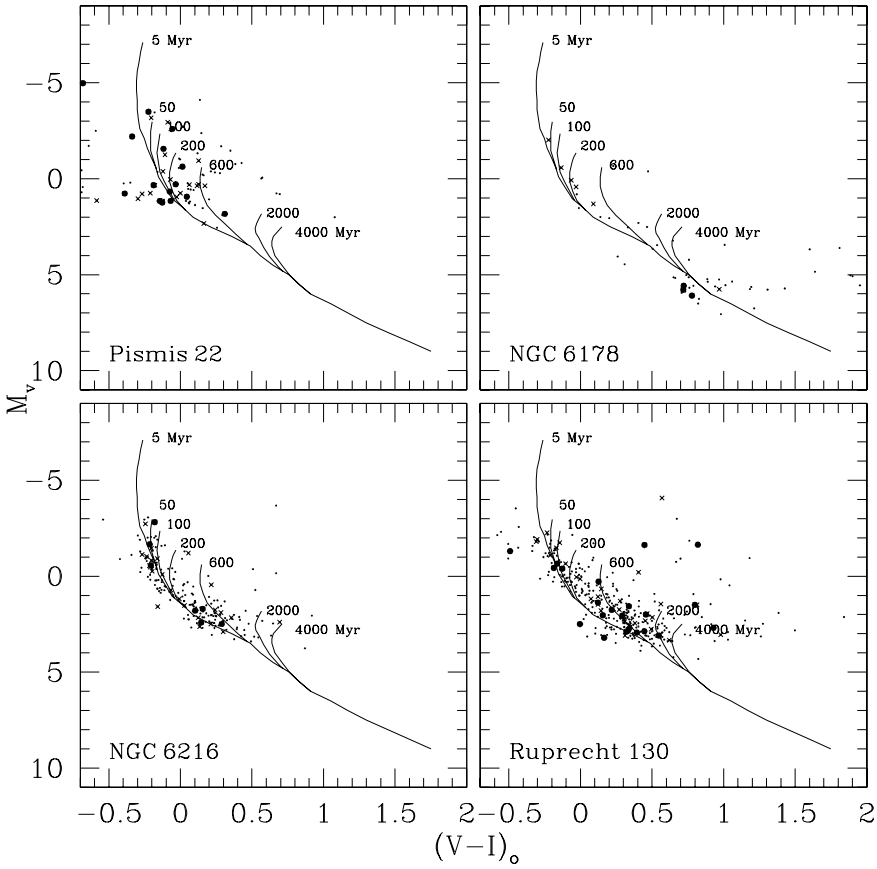

Fig. 4. M_v vs $(V\text{-}I)_o$ diagrams with the isochrones of Piatti et al. (1998c) superimposed. Symbols are as in Fig. 3.

1993, Ahumada et al. 2000). Indeed, Bica & Alloin (1986a) analized in detail integrated spectra of 63 known star clusters in the Large Magellanic Clouds and in our Galaxy. The sample included clusters embedded in HII regions throughout all ages up to those of globular clusters with a range of metallicities -2.1 $\leq$ [Fe/H] $\leq$ 0.1. They examined the behaviour of the equivalent widths for 70 spectral windows between 3780 and 7690 Å as well as the continuum distribution. From these data, they derived a grid of mean cluster properties as a function of age and metallicity. Bica & Alloin (1987) and Bica et al. (1990) performed a similar analysis for integrated spectra in the range 6400–9700 Å of 30 galactic clusters and 30 Large Magellanic Cloud clusters. More recently, Santos et al. (1995) examined the integrated spectral evolution in the blue-violet range of 97 blue clusters of the Magellanic Clouds, from very young objects associated with gas emission to older clusters with a few hundred Myr. As a result of these studies a library of template spectra is now available, which can be used to derive the fundamental parameters of the present cluster sample by comparing the observed cluster spectra with those of templates which most resemble them.

In Fig. 5 we present flux-calibrared integrated spectra of the observed clusters normalized to F_λ = 1 at λ = 6000 Å. Some amount of field star contamination may indeed be expected from stars located close to the cluster centres. However, only bright stars could affect the spectra significantly and this is not the case for either of the observed clusters. The spectra of Pismis 22

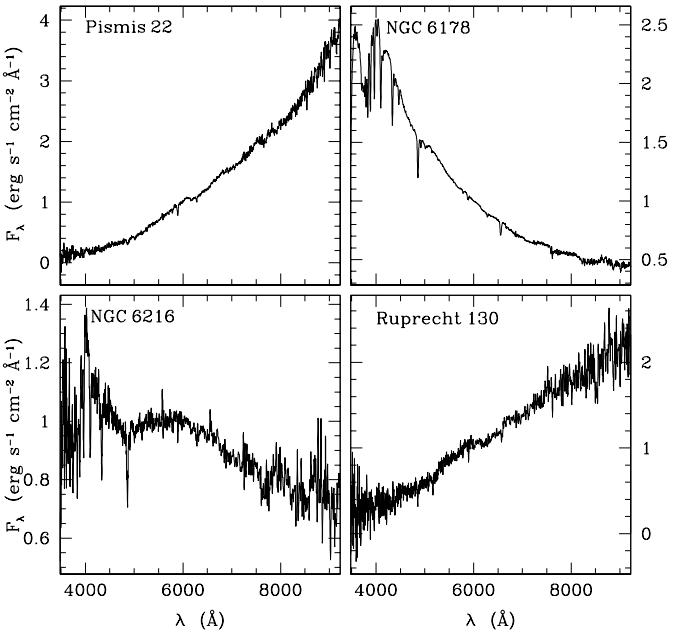

Fig. 5. Observed integrated spectra in absolute F_λ units normalized to F_λ = 1 at λ = 6000 Å.

and Ruprecht 130 are affected by a high interstellar absorption, as inferred from their pronounced positive continuum slope. If the positive slopes were caused by age -red giant stars should dominate the integrated light coming from the cluster- then,

Table 8. Cluster fundamental parameters derived from the spectroscopic analysis.

Cluster	W(Balmer) (Å)				Balmer-age	Template-age	E(B-V)
	Hα	Hβ	Hγ	Hδ	(Myr)	(Myr)	
Pismis 22	1.48±0.07	5.60±0.17	5.97±0.54	5.59±0.23	30±10	35–65	1.90
NGC 6178	4.94±0.24	5.37±0.16	5.67±0.51	7.53±0.30	50±25	3–6	0.20
NGC 6216	-2.00±0.10	5.93±0.18	6.76±0.61	6.47±0.26	40±8	12–40	0.45
Ruprecht 130	2.70±0.13	5.83±0.17	10.05±0.90	13.87±0.55	50±10	50	1.20

characteristic absorption features of red giants should appear in the cluster spectra, which is not the case for either of these two clusters. Therefore, we conclude that the integrated spectra of Pismis 22 and Ruprecht 130 correspond to those of relatively young clusters. The integrated spectrum of NGC 6216 also appears to be one of a young cluster. As seen, besides Balmer lines -Hα appears in emission- it is difficult to recognize metal lines, although the spectrum looks somewhat noisy.

To estimate reddening and age for the cluster sample, we first measured the equivalent widths (EWs) of the absorption Balmer lines and then interpolated those values into the age calibration obtained by Bica & Alloin (1986b, hereafter BA86b). To measure the EWs, we traced the continuum over the spectral region of the Balmer lines using the continuum flux points defined by BA86b and the SPLINE routine within the SPEED software (Schmidt 1988). We also defined some secondary flux points, especially around Hβ, if necessary. The EWs of the Balmer lines were measured in the spectral windows defined by BA86b. To estimate the uncertainties in the EW determinations, we traced two additional continua following the upper and lower envelopes of the spectra. The positions of the continuum flux points for these additional continua depended on the S/N ratio of each integrated spectrum. Finally, we compared the EW values for Hα, Hβ, Hγ and Hδ with Table II of BA86b and interpolated the corresponding reddening-independent ages. The dispersion in the age determinations from the different Balmer lines turned out to be less than 20% for NGC 6178 and NGC 6216, and 30% for Pismis 22. In the case of Ruprecht 130 we obtained an age dispersion lower than 15% after eliminating EW(Hδ), since Hδ is embedded in the continuun region with the lowest S/N ratio. The mean ages derived from Balmer lines are listed together with their estimated errors in Column (6) of Table 8.

We then selected template spectra with ages similar to the Balmer-line ages and compared different features of the cluster spectra with those of template spectra, particularly the continuum shape and the intensity of some lines. For that purpose, we changed the E(B-V) colour excess in a cluster spectrum using Seaton's (1979) absorption law, until we got the best match with the template spectrum which most resembles it. The templates YA (age $\approx$ 3–6 Myr), YC (12–40 Myr) and YDE (35–65 Myr) from Santos et al. (1995) were found to be particularly useful in the present study. We also used the template spectrum Y2 (50 Myr) from Bica (1988), which has a wider wavelength baseline. We recall that the cluster templates are not corrected for internal reddening and consequently the template matches provide foreground interstellar reddening. The template sequence essentially depends on age, the metallicity being negligible in the blue-visible range. Moreover, the blue-visible region is more sensitive to interstellar reddening and, therefore, plays a crucial role in the determination of the E(B-V) colour excess.

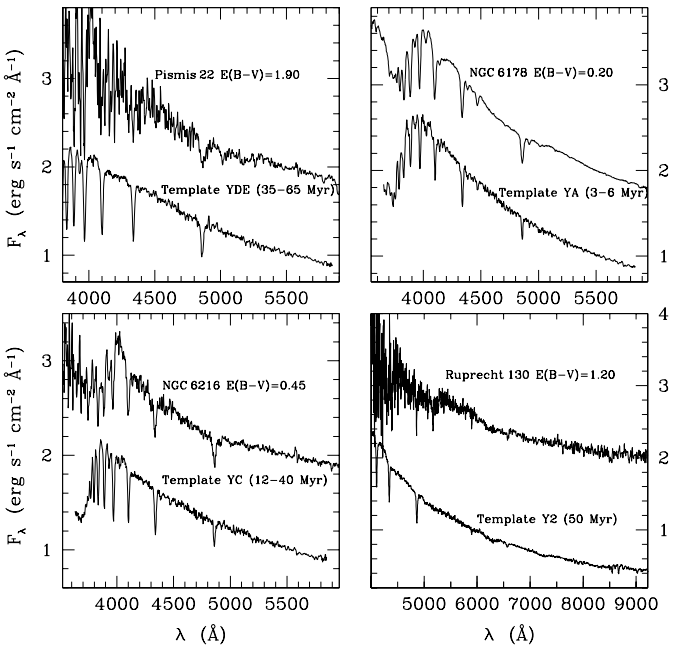

Fig. 6. Reddening-corrected integrated spectra compared with the template spectra which most resemble them. Cluster spectra were shifted by arbitrary constants for comparison purposes.

Fig. 6 shows the reddening corrected cluster spectra (top) compared with the template spectra which best match them (bottom). We added an arbitrary constant to the cluster spectra for comparison purposes. As shown in Fig. 6, the template spectrum we chose for each cluster satisfactorily reproduces the observed global and some particular features. In general, the continuum slope as well as the intensities of the Balmer lines present similar appearance in both spectra. Nevertheless, some differences can also be identified. In this respect, we recall that a template spectrum, built from the average of several integrated spectra, represents the combination of clusters distributed in a narrow age range and the statistics of contributing stars is high. On the other hand, an observed spectrum reflects the behaviour of the combined light of its members, so that eventual differences in the stellar population ratios may arise from stochastic effects in

Table 9. Adopted cluster fundamental parameters.

Cluster	E(B-V)	d (kpc)	Age (Myr)
Pismis 22	2.00±0.10	1.0±0.4	40±15
NGC 6178	0.20±0.05	1.3±0.2	40±10
NGC 6216	0.45±0.05	4.3±0.8	35±15
Ruprecht 130	1.20±0.05	2.1±0.4	50±10

poorly populated clusters or field star contamination. The age of the template which most resembles the cluster spectrum and the resulting E(B-V) colour excess are listed in Columns (7) and (8) of Table 8. The uncertainty in the reddening estimate is typically $\sim$ 0.05 mag.

5. Cluster parameters

The final cluster parameters were obtained by combining the results listed in Tables 7 and 8. The agreement found between the photometric and spectroscopic E(B-V) values is very good and, therefore, averaged E(B-V) values were finally adopted and listed in Table 9.

The adopted cluster ages basically correspond to those inferred from the spectroscopic analysis. These ages reflect the spectral synthesis of each cluster as a result of the light combination coming from different cluster stellar populations. Notice that both spectrocopic age estimates (see Table 8) show in general a satisfactory agreement and also are corroborated by the ages estimated from the isochrone-fitting. There exist, however, some differences in the spectroscopic ages. Such is the case of NGC 6178 for which we adopted the oldest value that agrees well with the photometric one. The highest S/N ratio in Table 1 corresponds to NGC 6178 so that the age derived from the Balmer EW's is an excellent age indicator in this case.

Cluster distances (d) were calculated from the adopted E(B-V) colour excess and apparent distance moduli listed in Table 7, using the ratio R = A_v/E(B-V) = 3.0 (Walker 1985, Straižys 1990). Distance uncentainties were estimated from the expression: σ(d) = 0.46[σ(V-M_v) + 3σ(E(B-V))]d, where σ(V-M_v) and σ(E(B-V)) represent the estimated errors in V-M_v and E(B-V), respectively. Table 9 summarizes for each cluster the fundamental parameters adopted and their estimated uncertainties. The adopted reddening and distance of NGC 6178 show a very good agreement with the values derived by MV73 as expected, since both the present photometry and MV73's are placed on the same magnitude scale. The cluster distance indicates that NGC 6178 is located foreground to the Ara OB1 association, as judged from the parameters of NGC 6193 (d = 1410 pc, $t \leq 3.1\times10^6$, Vázquez & Feinstein 1992), which is located at the centre of Ara OB1. NGC 6178 appears to be too old (age = 50 Myr) to be associated with Ara OB1. On the other hand, Pismis 22 also appears to be foreground to the star forming region to which the supernova remnant RCM 103 must be related to (d $\approx$ 6.6 kpc).

6. Conclusions

We present BVI CCD photometry for stars in the fields of the poorly studied or unstudied open clusters Pismis 22, NGC 6178, NGC 6216 and Ruprecht 130, projected not far from the Galactic centre ($331^\circ \leq l \leq 359^\circ$). The photometric data of NGC 6178 supersedes previous measurements by MV73. From the observed CMDs we confirmed the physical nature of the four objects as genuine open clusters and estimated their fundamental parameters. The clusters have well defined MSs which cover a range between 5 and 8 magnitudes in V, and are as faint as the 17^{th} down to the 19^{th} magnitude, depending on the cluster properties and exposure time. Reddenings, distances and ages were derived by fitting the fiducial cluster sequences with the ZAMS of Schmidt-Kaler (1982) and the empirical isochrones of Piatti et al. (1998c).

We also obtained flux-calibrated integrated spectra in the range 3500–9200 Å for the cluster sample and performed simultaneous estimates of age and foreground interstellar reddening by comparing the continuum distribution and line strengths of the cluster spectra with those of template cluster spectra with known parameters. The resulting photometric and spectroscopic values show very good agreement. The cluster sample includes objects with Galactocentric distances ranging between 1.0 kpc (NGC 6178) and 4.3 kpc (NGC 6216) from the Sun and their visual absorption range from $A_v \sim 0.6$ mag in NGC 6178 up to 6.0 mag in Pismis 22. The four studied objects are found to be young open clusters with ages between 35 and 50 Myr. Indeed, it would be interesting to have some metallicity estimations of these and other open clusters inside the solar radius in order to improve and enlarge our knowlegde of the chemical evolution of the Galactic disk, particularly towards the Galactic centre. It would be important to explore regions more centrally located in the Galactic disk, especially with the new generation of telescopes and instrumentation.

Acknowledgements. We wish to thank the Director, staff and technicians of CASLEO (Argentina) and Las Campanas Observatory for the allocation of observing time and for their kind assistance and hospitality. We also thank the referee T. von Hippel for his valuable comments and suggestions. We gratefully acknowledge financial support from the argentinian institutions CONICET, Agencia Nacional de Promoción Científica y Tecnológica (ANPCyT) and SECyT (National University of Córdoba) and the Brazilian Institution CNPq.

References

Ahumada A.V., Clariá J.J., Bica E., Piatti A.E., 2000, A&AS 141, 79
Bica E., 1988, A&A 195, 76
Bica E., Alloin D., 1986a, A&A 162, 21
Bica E., Alloin D., 1986b, A&AS 66, 171 (BA86b)
Bica E., Alloin D., 1987, A&A 186, 49
Bica E., Alloin D., Santos J.F.C., 1990, A&A 235, 103
Clariá J.J., Mermilliod J.C., Piatti A.E., 1999, A&AS 134, 301
FitzGerald M.P., Luiken M., Maitzen H.M., Moffat A.F.J., 1979, A&AS 37, 345
Gutiérrez-Moreno A., Moreno H., Cortés G., Wenderoth E., 1988, PASP 100, 973

Hagen G.L., 1970, An Atlas of Open Cluster Colour-Magnitude Diagrams. Publ. of the David Dunlap Observatory, University of Toronto
Ilovaisky A.S., Lequeux J., 1972, A&A 18, 169
Janes K.A., Tilley C., Lyngå G., 1988, AJ 95, 771
Kassis M., Friel E.D., Phelps R.L., 1996, AJ 111, 820
Landolt A.U., 1992, AJ 104, 340
Meynet G., Mermilliod J.C., Maeder A., 1993, A&AS 98, 477
Moffat A.F.J., Vogt N., 1973, A&AS 10, 135 (MV73)
Ng Y.K., Bertelli G., Chiosi C., Bressan A., 1996, A&A 310, 771
Piatti A.E., Clariá J.J., Abadi M.G., 1995, AJ 110, 2813
Piatti A.E., Bica E., Clariá J.J., 1998a, A&AS 127, 423
Piatti A.E., Clariá J.J., Bica E., Geisler D., Minniti D., 1998b, AJ 116, 801
Piatti A.E., Clariá J.J., Bica E., 1998c, ApJS 116, 263
Piatti A.E., Clariá J.J., Bica E., 1999, MNRAS 303, 65
Renzini A., Buzzoni A., 1985, In: Chiosi C., Renzini A. (eds.) Spectral Evolution of Galaxies. Reidel, Dordrecht, p. 195
Rosvick J.M., 1995, MNRAS 277, 1379
Santos J.F.C. Jr., Bica E., 1993, MNRAS 260, 915
Santos J.F.C. Jr., Bica E., Clariá J.J., et al., 1995, MNRAS 276, 1155
Schmidt A., 1988, User Manual. Federal University of Santa María, Brazil
Schmidt-Kaler Th., 1982, In: Schaifers K., Voigt H.H. (eds.) Landolt-Börnstein. Numerical Data and Functional Relationships in Science and Technology. New Series, group VI, Vol. 2b, Springer Verlag, Berlin
Seaton M.J., 1979, MNRAS 187, 73, short comm.
Stone R.P.S., Baldwin J.A., 1983, MNRAS 204, 347
Straižys V., 1990, Multicolor Stellar Photometry. Pachart Publ. House, Tucson, Arizona
Sung H., Bessell M.S., Lee S.W., 1998, AJ 115, 734
Twarog B.A., Ashman K.M., Anthony-Twarog B.J., 1997, AJ 114, 2556
van den Bergh S., 1978, ApJS 38, 119
Vázquez R.A., Feinstein A., 1992, A&AS 92, 863
Vázquez R.A., Baume G., Feinstein A., Prado P., 1996, A&AS 116, 75
Walker A.R., 1985, MNRAS 213, 889
Westerlund B.E., 1969, AJ 74, 882